

Short Communication

Preparation of Ni-TiO₂ Composite Coatings on Q390E Steel by Pulse Electrodeposition and their Photocatalytic and Corrosion Resistance Properties

Gang Zhao*, Mingtao Zhao and Weihua Zhang

Qingdao Huanghai University, Qingdao 266427, China

*E-mail: zhao_1980000@126.com

Received: 25 April 2022 / Accepted: 30 May 2022 / Published: 4 July 2022

Ni-TiO₂ composite coatings were prepared on the surface of Q390E steel by pulse electrodeposition. By investigating the effects of average current density, duty cycle and electrodeposition time on the TiO₂ particles content and the static contact angle of water droplet on the surface of the composite coating, the optimal process parameters of pulse electrodeposition were achieved and the optimized Ni-TiO₂ composite coating was obtained. The experimental results show that the optimized Ni-TiO₂ composite coating is uniform and compact, which is composed of small convex and irregular holes showing good hydrophobic performance with approximately 135° static contact angle of water droplet. After immersion in natural seawater for different times, the charge transfer resistance and low-frequency impedance values of the optimized Ni-TiO₂ composite coating gradually decrease and then basically maintains a constant trend, while the corrosion rate gradually increases and then also basically maintains a constant trend. The optimized Ni-TiO₂ composite coating shows good corrosion resistance which can provide ideal corrosion protection for Q390E steel in a long period.

Keywords: Ni-TiO₂ composite coating; Pulse electrodeposition; Photocatalytic; Corrosion resistance

1. INTRODUCTION

Q390E steel is commonly used in the manufacture of marine engineering equipments due to its good mechanical property, but its corrosion resistance is not ideal. Because of the special environment in which ocean engineering equipment is located, the most obvious characteristics are high salt solution, high humidity, dry and wet alternation and sea water splashing. The corrosion of Q390E steel will be accelerated by long-term exposure to various factors. In order to guarantee the reliability of ocean engineering equipments, corrosion protection is necessary for Q390E steel.

Some studies have confirmed that hot-dip galvanizing, electrodeposited alloy coatings and alumina coatings are a kind of simple and effective corrosion protection methods for steel, which can

achieve the effect of combining surface protection and surface strengthening [1-5]. Pure Zinc coating and zinc alloy coatings can effectively isolate water and chloride ions, so as to play a good role in corrosion protection of steel. Passivation is also a kind of simple and effective steel corrosion protection measures [6-9]. The passivation coating is dense and stable, which can effectively slow down the corrosion rate of steel. However, hot-dip galvanizing and its alloy coating process have high energy consumption and cost. Although the coating is thick, it is uneven with many surface defects. Passivation coatings are generally thin and cannot provide durable corrosion protection.

Electrodeposited nickel-based composite coatings possess the advantages of low energy consumption and cheap cost with uniform thickness, compact structure and good corrosion resistance, which are suitable for corrosion protection of steel. In recent years, more and more attentions have been paid to prepare nickel-based composite coatings [10-15]. In this paper, Ni-TiO₂ composite coatings were prepared on the surface of Q390E steel by pulse electrodeposition. By investigating the effects of average current density, duty cycle and electrodeposition time on the TiO₂ particles content and the static contact angle of water droplet on the surface of the composite coating, the optimal process parameters of pulse electrodeposition were optimized. The optimized Ni-TiO₂ composite coating was obtained and its anti-pollution performance and corrosion resistance was investigated.

2. EXPERIMENTAL

2.1 Pretreatment of Q390E steel

The Q390E steel plate with a thickness of 4 mm was selected for the experiment and cut into samples of 50 mm × 30 mm. The chemical composition of Q390E steel was as follows: 1.0~1.6% Mn, 0.7% Ni, 0.55% Si, 0.2% C, 0.3% Cr, 0.025% S, 0.025% P, the rest is Fe. The pretreatment process of Q390E steel samples is as follows: sandpaper polishing → abrasive polishing → chemical degreasing in alkaline solution (sodium hydroxide 40 g/L + sodium carbonate 12 g/L, 65°C) → activating in hydrochloric acid (volume fraction 10%, room temperature) → pure water cleaning → dry.

2.2 Preparation of Ni-TiO₂ composite coatings by pulse electrodeposition

After pretreatment, the Q390E steel sample and soluble nickel plate were used as the cathode and anode respectively. The spacing between the cathode and anode was set as 30 mm. The cathode and anode were placed parallel to each other, which were connected with the negative and positive poles of the pulse power supply respectively. The anode has at least twice the area of the cathode. The main composition of the plating solution were as follows: nickel aminosulfonate 400 g/L, nickel chloride 15 g/L, boric acid 40 g/L, sodium dodecyl benzene sulfonate 0.08 g/L and fluorinated TiO₂ particles (particle size of about 50 nm) 12 g/L. The beaker containing the plating solution was placed in the water bath of the ultrasonic cleaning machine to shake for 6 h and heated to 45°C at the same time to ensure the TiO₂ particles in the plating solution with a more evenly dispersed state. The process

parameters of pulse electrodeposition were as follows: average current density 1~5 A/dm², duty cycle 10~60%, electrodeposition time 8~60 min.

2.3 Performance testing of Ni-TiO₂ composite coatings

The Ni-TiO₂ composite coating samples were cleaned in anhydrous ethanol and deionized water successively. After being dried, the samples were cut for performance testing.

2.3.1 Surface morphology and composition

The morphology of Ni-TiO₂ composite coatings was observed by Quanta450 scanning electron microscope and the composition of Ni-TiO₂ composite coatings was analyzed by X-max 80 energy dispersive spectrometer. Based on the mass fraction of Ti element and the relative molecular weight relationship between Ti and TiO₂, the content of TiO₂ particles in the composite coating was calculated.

2.3.2 Static contact angle

JC2000D1 type contact angle measuring instrument was used to measure the static contact angle of water droplet on the surface of Ni-TiO₂ composite coatings. The droplet volume was 4 μL and dropped randomly at three different positions on the surface of the samples. The measurement results were averaged to reduce the error.

2.3.3 Photocatalytic properties

Soot was selected as a simulated solid pollutant and spread evenly on the surface of the Ni-TiO₂ composite coating samples which was placed at an inclination of 10°. A syringe was used to drop water on the top of the sample to observe the influence of water droplet moving along the inclined direction on the surrounding soot. The anti-pollution performance of Ni-TiO₂ composite coatings was evaluated.

The Ni-TiO₂ composite coating samples were immersed in methylene blue solution to simulate liquid pollutants and irradiated by ultraviolet light-emitting diode. The samples absorb ultraviolet light to reduce the absorbance of the solution. From the beginning to the end of the reaction, the absorbance of the solution was measured by UV2550 spectrophotometer every 30 min. This value is related to the degradation rate of methylene blue by Ni-TiO₂ composite coatings under the action of ultraviolet photocatalysis shown in equation 1, and it can be used to evaluate the photocatalytic properties of Ni-TiO₂ composite coatings.

$$D = \frac{A_{\text{begin}} - A_{\text{end}}}{A_{\text{begin}}} \times 100\% \quad (1)$$

Where, D represents methylene blue degradation rate, A_{begin} and A_{end} represent initial and end absorbance of the solution respectively.

2.3.4 Corrosion resistance

The electrochemical impedance spectra of Ni-TiO₂ composite coating immersed in natural seawater for different time was measured by CHI660D electrochemical workstation. Moreover, the electrochemical impedance spectra of Q390E steel was also measured as comparison. Working electrode was the test sample, reference electrode was the saturated calomel electrode and auxiliary electrode was the platinum sheet. 5 mV disturbance potential was applied during the test, and the frequency range was 100 kHz~10 mHz.

In addition, the Q390E steel and Ni-TiO₂ composite coating samples were immersed in natural seawater for different days respectively, and the corrosion rate was tested by weight loss method.

$$V_{\text{corr}} = \frac{\Delta G}{S \cdot t} \quad (2)$$

Where, V_{corr} represents the corrosion rate, the unit is mg/(cm²·d); ΔG represents the corrosion weight loss, the unit is mg; S represents the surface area of the sample, the unit is cm²; t represents the immersion time, the unit is d.

3. RESULT AND DISCUSSION

3.1 Effects of pulse electrodeposition parameters on TiO₂ particles content and static contact angle

Figure 1 shows the TiO₂ particles content and static contact angle of water droplet of the Ni-TiO₂ composite coatings electrodeposited at different average current density. It can be seen from Figure 1 that with the increase of average current density from 1 A/dm² to 5 A/dm², TiO₂ particles content increases from 7.13% to 10.52% and then decreases to 6.78%. According to the adsorption theory, Ni²⁺ can be physically adsorbed on the surface of TiO₂ particles and migrate to the deposition surface under the attraction of the electric field [16-18]. The increase in average current density makes the electric field more attractive to the positively charged TiO₂ particles, driving more particles to be encapsulated in the coating. Since the surface energy of the fluorinated TiO₂ particles is very low, the dispersion state in the composite coating can reduce the surface free energy, weaken the affinity of the composite coating to water droplet, and hinder the spreading of water droplet. In addition, the increased TiO₂ particles content is conducive to the formation of a special structure on the surface of the composite coating, thereby changing the static contact angle of water droplet. Hydrophobic performance of TiO₂ is investigated in many papers [19-21]. However, when average current density exceeds a certain range, a serious hydrogen evolution reaction will occur, which hinders the migration of TiO₂ particles to the deposition surface, so that the TiO₂ particles content of the composite coating decreases resulting in the decrease of static contact angle.

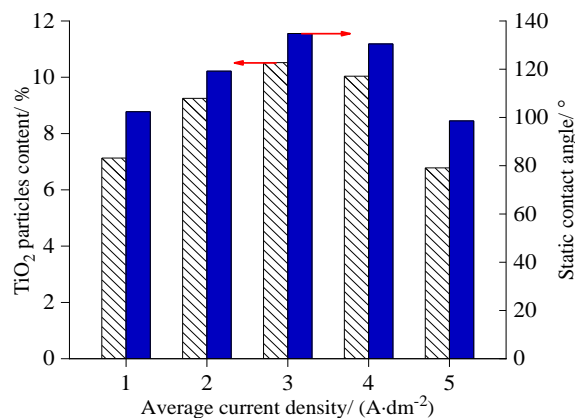


Figure 1. TiO₂ particles content and static contact angle of water droplet of the Ni-TiO₂ composite coatings electrodeposited at different average current density

Figure 2 shows the TiO₂ particles content and static contact angle of water droplet of the Ni-TiO₂ composite coatings electrodeposited under different duty cycle. Some people also study the effect of duty cycle on metal coating or composite coating during the pulse electrodeposition [22-24]. As can be seen from Figure 2, with the increase of duty cycle from 10% to 60%, TiO₂ particles content presents an increasing trend, accompanied by a gradual increase in the static contact angle. The reason is that when duty cycle is low, the current conduction time is short, which is equivalent to electrodeposition under low current density, so that the electric field has weak attraction to positively charged TiO₂ particles, resulting in fewer particles in the coating. In this case, the surface free energy of the composite coating is higher, and the surface does not form a special structure, so the static contact angle is larger. With the increase of duty cycle, the current conduction time is prolonged and the turn-off time is shortened, which is equivalent to electrodeposition under high current density. The enhancement of electric field force attracts more TiO₂ particles to be co-deposited in the coating, which reduces the surface free energy of the composite coating. At the same time, it is also conducive to the formation of special structure on the surface of the composite coating, which hinders the spread of water droplet and increases the static contact angle.

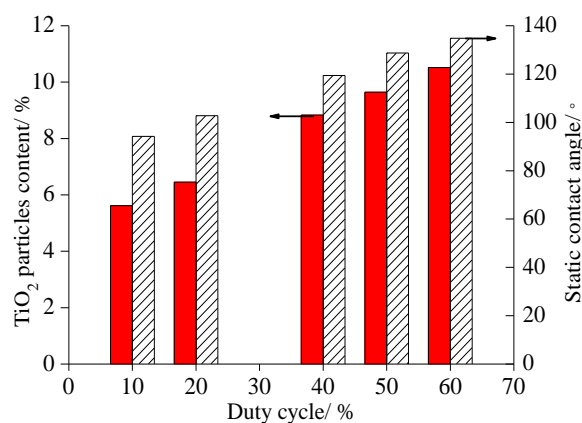


Figure 2. TiO₂ particles content and static contact angle of water droplet of the Ni-TiO₂ composite coatings electrodeposited under different duty cycle

Figure 3 shows the TiO₂ particles content and static contact angle of water droplet of the Ni-TiO₂ composite coatings electrodeposited at different electrodeposition time. It can be seen from Figure 3 that with the prolongation of electrodeposition time from 8 min to 60 min, TiO₂ particles content tends to increase and the static contact angle increases firstly and then tends to a constant value. The reason is that the prolongation of electrodeposition time makes the composite coating gradually thicker and form a Ni-TiO₂ composite coating with higher particles content and low surface free energy. In addition, the dispersed distribution of more particles is conducive to the formation of a special structure on the surface of the composite coating, which reduces the contact area with water droplet and hinders the spread of water droplet, thus showing a larger static contact angle. Continuing to prolong electrodeposition time, although the composite coating continues to thicken and the TiO₂ particles content increases, the static contact angle does not further increase. The reason may be that the TiO₂ particles content reaching a certain limit has no significant effect on the surface free energy of the composite coating.

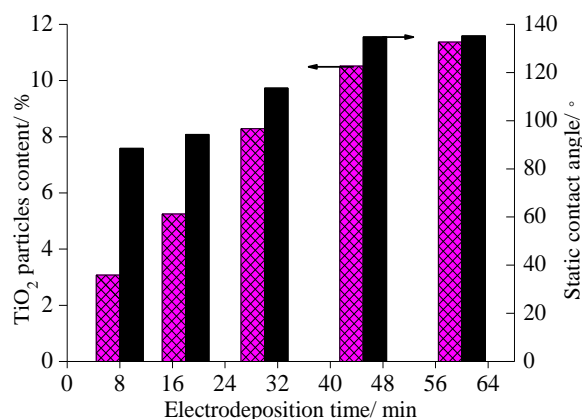


Figure 3. TiO₂ particles content and static contact angle of water droplet of the Ni-TiO₂ composite coatings electrodeposited at different electrodeposition time

In conclusion, when the average current density is 3 A/dm², duty cycle is 60% and electrodeposition time is 45 min, TiO₂ particles content of the electrodeposited Ni-TiO₂ composite coating (named as optimized Ni-TiO₂ composite coating) reaches 10.52%, and the static contact angle of water droplet is close to 135°, indicating that the optimized Ni-TiO₂ composite coating shows good hydrophobic performance. Figure 4 shows the surface morphology of the optimized Ni-TiO₂ composite coating and the shape of water droplet on its surface. It can be seen that the optimized Ni-TiO₂ composite coating is relatively uniform and compact, and a special structure composed of micro-raised and irregular holes is formed. Water droplet on the surface of this special structure presents an excellent arc shape. The optimized Ni-TiO₂ composite coating is taken as the research object to analyze the anti-pollution performance and corrosion resistance.

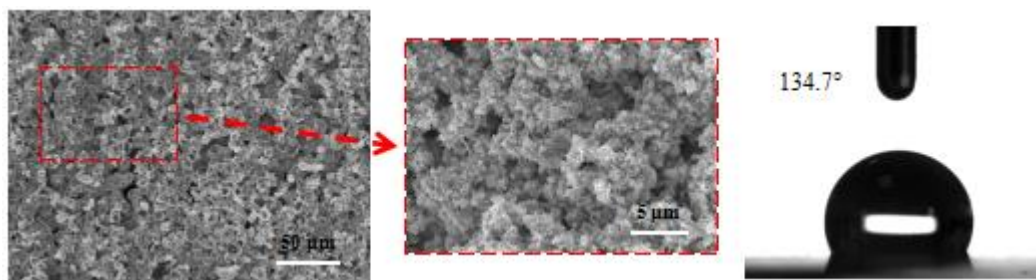


Figure 4. Surface morphology of optimized Ni-TiO₂ composite coating and the shape of water droplet on its surface

3.2 Photocatalytic properties of optimized Ni-TiO₂ composite coating

Figure 5 shows the morphology of water droplet on the surface of Q390E steel and the optimized Ni-TiO₂ composite coating spread with soot. It can be seen from Figure 5(a) that water droplet adhering to the surface of Q390E steel do not roll down along the inclined direction, and shows an arc shape, gathering the surrounding soot. Because the surface of Q390E steel is hydrophilic and soot is also hydrophilic, which does not has anti-pollution performance. It can be seen from Figure 5(b) that water droplet on the surface of the optimized Ni-TiO₂ composite coating roll down along the inclined direction, and the shape of water droplet is basically unchanged during the rolling process. And as the water droplet fall, it carries soot on the surface and clears a clean track, which is clearly distinct from the surrounding area. Because the surface of the optimized Ni-TiO₂ composite coating presents good hydrophobic performance with low surface free energy which is not easy to adhere to soot, even the soot can be cleaned by falling water droplet. It can be inferred that the optimized Ni-TiO₂ composite coating has good anti-pollution performance and it can effectively prevent Q390E steel from being polluted.

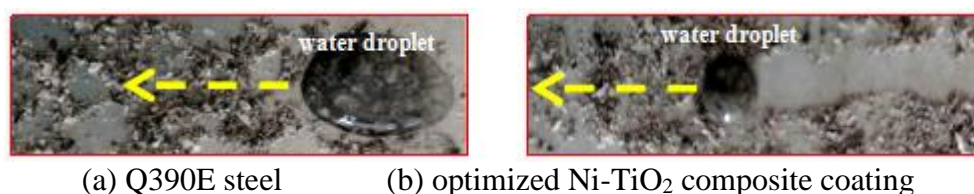


Figure 5. Morphology of water droplet on the surface of Q390E steel and the optimized Ni-TiO₂ composite coating

Figure 6 shows the absorbance variation trend of Q390E steel and the optimized Ni-TiO₂ composite coating immersed in methylene blue solution for 150 min. When Q390E steel is immersed in methylene blue solution, the absorbance changes slightly with the extension of immersion time. This indicates that the surface photocatalytic property of Q390E steel is very weak, and it is difficult to degrade the adsorption of methylene blue on the surface under ultraviolet photocatalytic action. The

absorbance of the optimized Ni-TiO₂ composite coating in methylene blue solution varies greatly with the extension of immersion time. These results indicate that the surface of the optimized Ni-TiO₂ composite coating has photocatalytic property, which can degrade the adsorption of methylene blue on the surface under the ultraviolet photocatalytic action, resulting in the reduction of the solution absorbance. The reason is that the optimized Ni-TiO₂ composite coating contains more TiO₂ particles with strong absorption capacity of ultraviolet light. When irradiated by ultraviolet light, TiO₂ particles will generate hydroxyl radicals and superoxide radicals with strong oxidation capacity [25-26]. Under the synergistic effect of various active substances such as electrons, holes, hydroxyl radicals and superoxide radicals, methylene blue is degraded into carbon dioxide, water molecules and harmless inorganic substances.

According to the absorbance variation trend of solution, the degradation rate of Q390E steel and the optimized Ni-TiO₂ composite coating to methylene blue are 4.3% and 17.4%, respectively. This indicates that the methylene blue adsorbed on the surface of Q390E steel can hardly be degraded, while the methylene blue adsorbed on the surface of the optimized Ni-TiO₂ composite coating is degraded to a certain extent. It is generally believed that the higher the degradation rate of methylene blue, the better the photocatalytic properties of the material surface. More TiO₂ particles are dispersed and distributed in the optimized Ni-TiO₂ composite coating, showing the ability to absorb ultraviolet light. Under the synergistic effect of various active substances generated by ultraviolet light irradiation, the methylene blue adsorbed on the surface of the optimized Ni-TiO₂ composite coating can be degraded, thus showing decent photocatalytic properties. It has been reported that the TiO₂ particles, TiO₂ coating and TiO₂ composite coating all have good photocatalytic property [27-29].

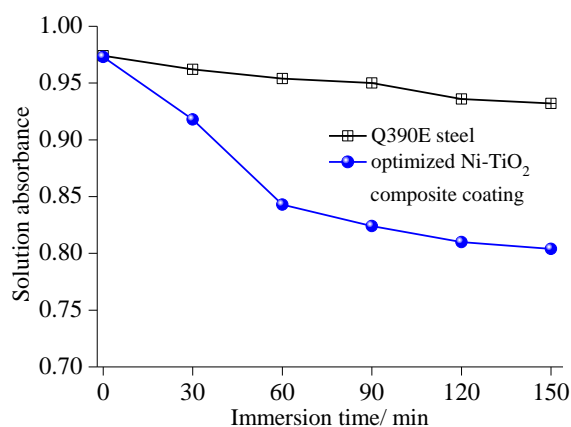


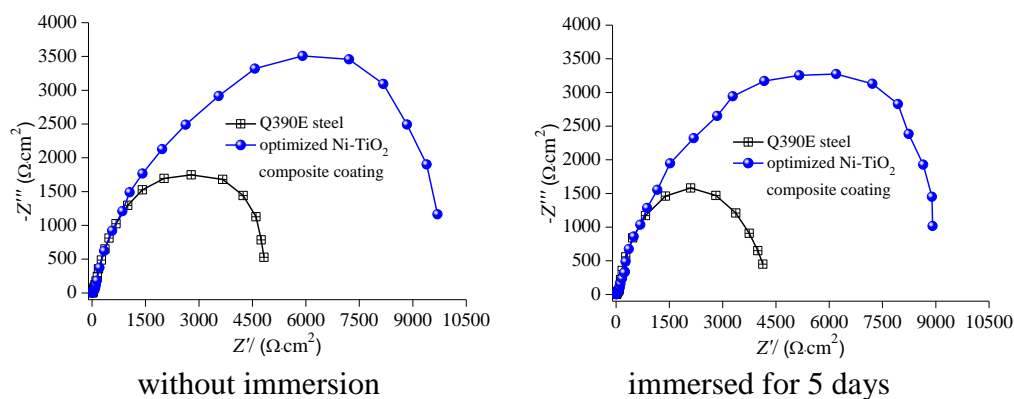
Figure 6. Absorbance variation trend of Q390E steel and the optimized Ni-TiO₂ composite coating immersed in methylene blue solution for 150 min

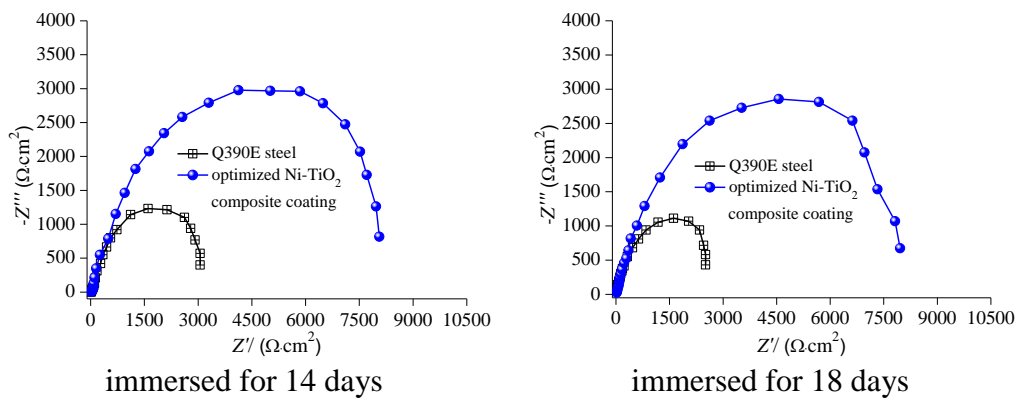
3.3 Corrosion resistance of optimized Ni-TiO₂ composite coating

Figure 7 shows the electrochemical impedance spectra of Q390E steel and the optimized Ni-TiO₂ composite coating immersed in natural seawater for different time. As can be seen from Figure 7(a), without immersion, the arc radius of the optimized Ni-TiO₂ composite coating is much larger

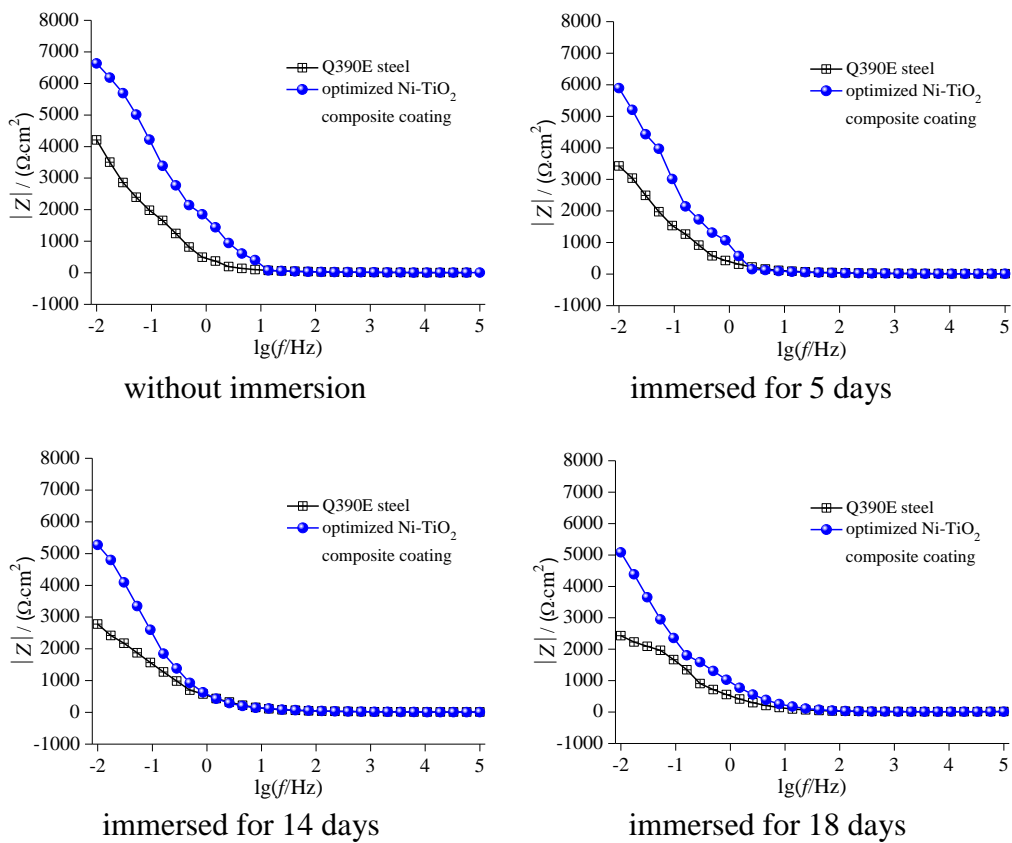
than that of Q390E steel, and the charge transfer resistance is about $4580 \Omega \cdot \text{cm}^2$, which is two times larger than that of Q390E steel, as shown in Figure 8. After immersion in natural seawater for 5 days, 14 days and 18 days, the arc-shaped of the optimized Ni-TiO₂ composite coating is still relatively regular (approximately semi-circular), indicating that the composite coating continues to provide protection for Q390E steel. However, with the extension of immersion time, the arc radius of Q390E steel decreases gradually, and the charge transfer resistance decreases linearly from $2460 \Omega \cdot \text{cm}^2$ to $1230 \Omega \cdot \text{cm}^2$, indicating that the corrosion degree of Q390E steel increases and its corrosion resistance decreases significantly. The arc radius of the optimized Ni-TiO₂ composite coating first decreases and then remains basically unchanged while the charge transfer resistance decreases slowly from $4580 \Omega \cdot \text{cm}^2$ to $3970 \Omega \cdot \text{cm}^2$ and then keep stable. The slow decrease of the charge transfer resistance indicates that the corrosion resistance of the optimized Ni-TiO₂ composite coating decreases, but the basically constant charge transfer resistance indicates that the corrosion resistance of the optimized Ni-TiO₂ composite coating maintains a stable state.

As can be seen from Figure 7(b), without immersion, the relationship between impedance value $|Z|$ and frequency of the optimized Ni-TiO₂ composite coating is similar to that of Q390E steel. Some studies have shown that low frequency impedance value $|Z|_{0.01 \text{ Hz}}$ can reflect the block effect of the coating for corrosive medium [30-31]. Without immersion, $|Z|_{0.01 \text{ Hz}}$ of the optimized Ni-TiO₂ composite coating is about $6640 \Omega \cdot \text{cm}^2$, which is 1.5 times larger than that of Q390E steel, as shown in Figure 9. After immersion in natural seawater for 5 days, 14 days and 18 days, $|Z|_{0.01 \text{ Hz}}$ of the optimized Ni-TiO₂ decreases slowly and basically remain unchanged. However, $|Z|_{0.01 \text{ Hz}}$ of the Q390E steel shows the tendency of decreased significantly. This further indicates that the optimized Ni-TiO₂ composite coating has good corrosion resistance. The reason is that the optimized Ni-TiO₂ composite coating has good hydrophobic performance, which can capture air to fill the special structure formed on the surface and effectively prevent the contact between corrosive media such as chloride ions and the surface. In addition, more TiO₂ particles are dispersed and distributed in the optimized Ni-TiO₂ composite coating, which plays a role of dispersion strengthening and also prevents the infiltration of corrosive medium into the coating to a certain extent, thus showing excellent corrosion resistance. It can provide ideal corrosion protection for Q390E steel in a long period.





(a) Nyquist spectra



(b) Bode spectra

Figure 7. Electrochemical impedance spectra of Q390E steel and the optimized Ni-TiO₂ composite coating immersed in natural seawater for different time

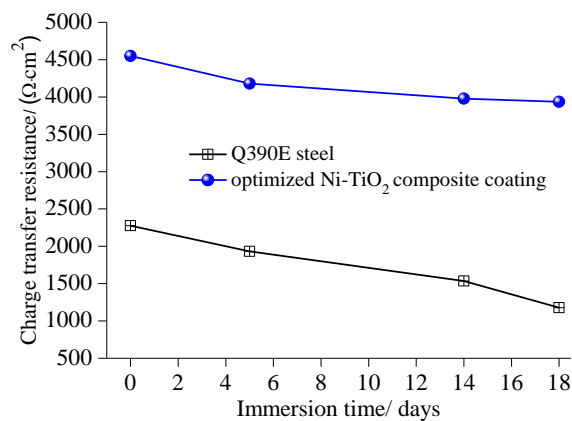


Figure 8. Variation trend of charge transfer resistance of Q390E steel and the optimized Ni-TiO₂ composite coating

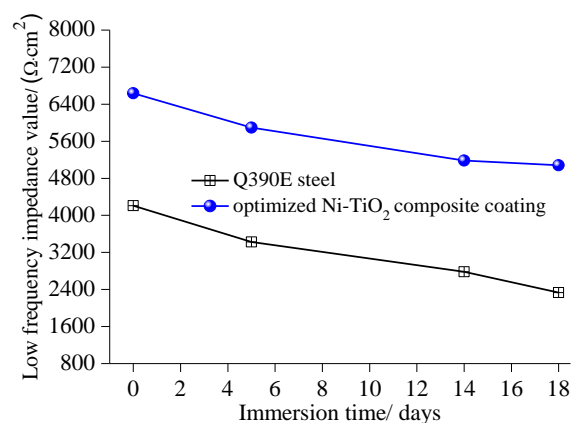


Figure 9. Variation trend of low frequency impedance value of Q390E steel and the optimized Ni-TiO₂ composite coating

Figure 10 shows the corrosion rate variation trend of Q390E steel and the optimized Ni-TiO₂ composite coating immersed in natural seawater for different time. The corrosion rate of Q390E steel firstly increases significantly and then increases slowly after immersion in natural seawater for 14 days, while the corrosion rate of the optimized Ni-TiO₂ composite coating increases slowly and maintains stable after immersion in natural seawater for 14 days. After immersion in natural seawater more than 14 days, the corrosion rate of the optimized Ni-TiO₂ composite coating increases very little. This indicates that the corrosion degree is relatively light at this stage, and the corrosion resistance remains in a stable state due to a dense corrosion products film is formed on the surface [32-33]. The reason is that the optimized Ni-TiO₂ composite coating is relatively uniform and compact. It has good hydrophobic performance, which can effectively prevent the contact of corrosive ions such as chloride ions with the surface, thus reducing the corrosion degree, and it can provide good corrosion protection for Q390E steel.

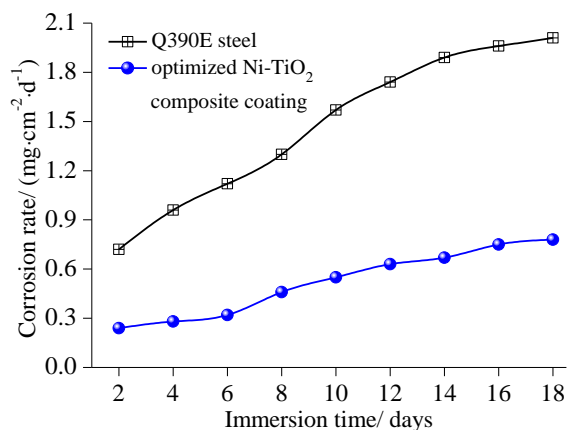


Figure 10. Corrosion rate variation trend of Q390E steel and the optimized Ni-TiO₂ composite coating immersed in natural seawater for different time

4. CONCLUSIONS

(1) Average current density, duty cycle and electrodeposition time have a certain influence on the TiO₂ particles content and static contact angle of water droplet of Ni-TiO₂ composite coatings. The optimal process parameters of pulse electrodeposition are as follows: average current density 3 A/dm², duty cycle 60%, electrodeposition time 45 min. TiO₂ particles content of the optimized Ni-TiO₂ composite coating reaches 10.52%, and the static contact angle of water droplet on its surface is close to 135°. The optimized Ni-TiO₂ composite coating possesses good hydrophobic performance, as well as decent anti-pollution performance and good corrosion resistance.

(2) Compared with Q390E steel, the charge transfer resistance and low-frequency impedance of the optimized Ni-TiO₂ composite coating increase sharply. The surface of the optimized Ni-TiO₂ composite coating has photocatalytic property, which can degrade the methylene blue adsorbed on the surface under the action of ultraviolet. The optimized Ni-TiO₂ composite coating can provide good corrosion protection for Q390E steel, and it can prevent Q390E steel from being polluted.

References

1. G. S. Sharma, M. Sugavaneswaran, U. Vijayalakshmi and R. Prakash, *Ceram. Int.*, 45 (2019) 13456.
2. Y. Adraider, Y. X. Pang, F. Nabhani, S. N. Hodgson, M. C. Sharp and A. Al-Waidh, *Ceram. Int.*, 40 (2014) 6151.
3. X. S. Lv, Y. Qin, H. Liang, B. X. Zhao, Y. He and X. M. Cui, *Appl. Surf. Sci.*, 562 (2021) 150192.
4. R. Tavangar, R. Naderi and M. Mahdavian, *Prog. Org. Coat.*, 158 (2021) 106384.
5. A. Kumar, S. K. Bholra and J. D. Majumdar, *Surf. Coat. Technol.*, 206 (2012) 3693.
6. W. B. Du, C. J. Liu and Y. Y. Yue, *Corros. Sci.*, 22 (2022) 110318.
7. Q. Guo, X. Z. Li, Y. L. Song and J. Z. Liu, *Case Stud. Constr. Mater.*, 16 (2022) 00892.
8. J. K. Singh, H. M. Yang, H. S. Lee, S. Mandal, F. Aslam and R. Alyousef, *J. Mol. Liq.*, 337 (2021) 116454.

9. P. Xu, L. H. Jiang, M. Z. Guo, J. Zha, L. Chen, C. Chen and N. Xu, *Constr. Build. Mater.*, 223 (2019) 352.
10. M. Alizadeh and H. Safaei, *Appl. Surf. Sci.*, 456 (2018) 195.
11. S. Singh, S. Samanta, A. K. Das and R. R. Sahoo, *Surf. Interfaces*, 12 (2018) 61.
12. F. F. Xia, W. C. Jia, C. Y. Ma and J. Wang, *Ceram. Int.*, 44 (2018) 766.
13. E. Unal and I. H. Karahan, *J. Alloys Compd.*, 763 (2018) 329.
14. A. Goral and S. J. Skrzypek, *Appl. Surf. Sci.*, 456 (2018) 147.
15. E. Beltowska-Lehman, A. Bigos, P. Indyka, A. Chojnacka, A. Drewienkiewicz, S. Zimowski, M. Kot and M. J. Szczerba, *J. Electroanal. Chem.*, 813 (2018) 39.
16. W. Lamouchi, S. B. Slama, F. Saadallah and M. Bouaicha, *Optik*, 227 (2021) 166123.
17. S. F. Blaskiewicz, H. L. S. Santos, I. F. Teixeira, J. L. Bott-Neto, P. S. Fernandez and L. H. Mascaro, *Mater. Today Nano*, 18 (2022) 100192.
18. A. H. Barros, N. B. Castro, A. V. Ortiz, C. T. Tovar and A. D. G. Delgado, *Sustainable Chem. Pharm.*, 17 (2020) 100299.
19. Q. Tang, W. Chen, X. N. Dai, Y. C. Liu, H. Liu, L. Q. Fan, H. B. Luo, L. Ji and K. Zhang, *Chemosphere*, 263 (2021) 128066.
20. F. Dogan and H. Dehghanpour, *J. Build. Eng.*, 40 (2021) 102689.
21. Y. L. Xi, Y. L. Qi, Z. P. Mao, Z. B. Yang and J. Zhang, *Constr. Build. Mater.*, 266 (2021) 120916.
22. Y. D. Yu, G. Y. Wei, H. F. Guo, J. W. Lou and H. L. Ge, *Surf. Eng.*, 28 (2012) 30.
23. Z. Q. Fu, Z. L. Miao, W. Yue, C. B. Wang, J. J. Kang, L. N. Zhu and Z. J. Peng, *Rare Met. Mater. Eng.*, 47 (2018) 3482.
24. Y. Q. Wei and C. Z. Gong, *Appl. Surf. Sci.*, 257 (2011) 7881.
25. J. J. Wu, J. X. Hao, W. Y. Guo, J. Chen and Y. L. Min, *J. Colloid Interface Sci.*, 613 (2022) 616.
26. M. Ge, Z. Hu, J. L. Wei, Q. B. He and Z. X. He, *J. Alloys Compd.*, 888 (2021) 161625.
27. S. Y. Kim, B. J. Cha, S. F. Zhao, H. O. Seo and Y. D. Kim, *Constr. Build. Mater.*, 296 (2021) 123763.
28. H. Khatibnezhad, F. Ambriz-Vargas, F. B. Ettouil and C. Moreau, *J. Eur. Ceram. Soc.*, 42 (2022) 2905.
29. R. M. Hou, Y. Jia, F. Wang, D. Huang, X. M. Lv and H. Y. Wang, *Diamond Relat. Mater.*, 126 (2022) 109107.
30. V. Renciukova, J. Macak, P. Sajdi, R. Novotny and A. Krausova, *J. Nucl. Mater.*, 510 (2018) 312.
31. M. D. D. Ayagou, T. T. M. Tran, B. Tribollet, J. Kittel, E. Sutter, N. Ferrando, C. Mendibide and C. D. Thual, *Electrochim. Acta*, 282 (2018) 775.
32. W. C. Kong, K. M. Li and J. Hu, *Int. J. Hydrogen Energy*, 47 (2022) 6911.
33. M. Mobin, M. Parveen and R. Aslam, *J. Phys. Chem. Solids*, 161 (2022) 110422.